Characterization of surface anchoring energy of nematic liquid crystals via electrohydrodynamic instability

Dae Geon Ryu,[1] Jong-Hoon Huh,[2] Young-Ki Kim,[3,*] and Jin Seog Gwag[1,†]

[1]*Department of Physics, Yeungnam University, 280 Daehak-Ro, Gyeongsan 38541, Republic of Korea*

[2]*Department of Mechanical Information Science and Technology, Faculty of Computer Science and Systems Engineering, Kyushu Institute of Technology, Iizuka, Fukuoka 820–8502, Japan*

[3]*Department of Chemical Engineering, Pohang University of Science and Technology, 67 Cheongam-ro, Pohang, Gyeongbuk 37673, Republic of Korea*

(Received 22 January 2020; revised manuscript received 25 May 2020; accepted 27 May 2020; published 18 June 2020)

Herein, a method is proposed to determine the azimuthal anchoring energies of surface liquid crystals (LCs), as they gradually change orientation from a vertical to a horizontal state owing to an increase in the voltage applied to each LC cell. The LC cells are characterized using the direction of the Williams roll pattern related to the midplane LC director of the conduction regime of the electrohydrodynamic convection patterns of LCs. The application of the midplane LC directions, obtained from the direction of the roll patterns, to the Ericksen-Leslie equation produces the precise values of the surface anchoring strength. The hybrid type 90°-twisted nematic LC cell, composed of homeotropic and homogeneous LC alignment layers on the top and bottom substrates, respectively, was used to find the azimuthal anchoring energy of the surface LCs, indicated by voltages at the initially vertically aligned LC state. It was observed that the surface azimuthal anchoring energy on the homeotropic layer increased with an increase in voltage. We expect that the proposed technique may be excellent in terms of ease of use, simplicity, and accuracy because the azimuthal anchoring energy can be visually evaluated through the roll pattern.

DOI: 10.1103/PhysRevE.101.062703

I. INTRODUCTION

Nematic liquid crystals (LCs) are complex fluids with a long-range orientational ordering of molecules, defined as a director **n**, resulting in anisotropic mechanical and optical properties (e.g., elasticity, birefringence) [1,2]. Therefore, LCs has an ability to transform their interfacial and internal characteristics via the reorientation of **n** in response to external forces. This unique capability has provided a basis for design of stimuli-responsive LC materials that are finding applications in a variety of fields, including light modulators, actuators, sensing, photonics, and drug release [3–12]. In the design of responsive LC materials, interfacial characterization of LCs is crucially important because the initial orientation of surface LCs defines their interfacial behavior in response to stimuli, which in turn influences the internal ordering of LCs [3–5,13]. For a representative nematic LC, 4′-pentyl-4-biphenylcarbonitrile (5CB), for instance, a horizontal orientation of **n** (planar surface anchoring) is imposed at the LC-aqueous interface or solid interface coated with polymers, while the LC-air interface causes a vertical orientation (homeotropic surface anchoring). The LC interfaces can be designed to make an orientational transition of surface LCs from the initial surface anchoring and signal the change into a macroscopic optical output upon an application of targeted triggers, including electric/magnetic field [1,2,7–9], self-assembly of chemical species [3–6], mechanical stress [6,7], and UV or temperature [6,9–11]. To this end, therefore, the surface property of LCs to resist deviation of **n** from the initial anchoring, which is described by a surface anchoring energy, needs to be fully understood as it can be programmed to control the interfacial LC behaviors (e.g., selectivity, sensitivity, and responsivity) and thus be a key factor to provide insight into the rational design of responsive LC systems. Accordingly, previous studies have proposed a number of methods to determine the azimuthal (W) [14–19] and polar anchoring energies (U) of LCs at surfaces [20–25]. For the measurement of the azimuthal anchoring energy, in particular, most of previous studies are limited to the horizontally aligned LC systems in which W has been determined by characterizing optically the deviation angles of surface LCs from the lowest free energy orientation of **n** (so-called easy axis), which is typically set by surface rubbing. In contrast, there has been little research done in measuring W in the vertically aligned LC systems although the vertical alignment has been also adopted in a wide range of responsive LC systems.

Herein, we propose a facile, but highly accurate method to measure the azimuthal anchoring energy of LCs at homeotropic alignment surfaces by characterizing the orientation of so-called "roll pattern" derived from electrohydrodynamic convection (EHC). In LCs with an opposite sign of dielectric and conductive anisotropy, an electric fields ($\boldsymbol{E}$)

*Corresponding author: ykkim@postech.ac.kr
†Corresponding author: sweat3000@ynu.ac.kr

applied across the LC films can cause internal motion of electrical charges, leading to electrohydrodynamic instability with various LC convection patterns [26–32]. Specifically, the roll pattern (also known as Williams domain) resulting from Carr-Helfrich instability appears at a low-frequency conductive regime [32–36]. Interestingly, the previous studies found the orientation of roll patterns to be defined perpendicular to **n** at the midplane of twisted LC cell where **n** rotates across the LC film [33–36]. Therefore, one can simply determine the midplane **n** ($\mathbf{n}_\mathrm{m}$) by observing the direction of induced roll pattern under an optical microscope. When **n** are twisted by ϕ across the LC film (along the z direction) confined between top and bottom surfaces with identical W,$\mathbf{n}_\mathrm{m}$ is always set by $\phi/2(=\phi_m(z=d/2))$;$\phi(z=d)=\phi$ and $\phi(z=0)=0$, where d is the thickness of LC film. For the LC cell with asymmetric anchoring boundaries, however, $\mathbf{n}_\mathrm{m}$ tend to lean towards the easy axis at the surface with stronger W, deviating from $\phi/2$ due to the competition between surface anchoring energy and bulk elastic energy [14–19]. $\mathbf{n}_\mathrm{m}$ can be determined by the torque balance equation, thus facilitating the determination of W. By leveraging this correlation of the roll pattern with W, we present in this paper the facile method to determine the azimuthal anchoring energy of surfaces with the homeotropic anchoring.

II. THEORETICAL BACKGROUND

In this section, we present the theoretical principle for determining an unknown surface anchoring energy, by measuring the orientation of $\mathbf{n}_\mathrm{m}$ in LC cells. In this work, the evaluation was done with the LC cell in which W of one substrate is known.

The free energy density in the LC film in terms of $\mathbf{n}=(n_x,n_y,n_z)$ [1,2] is given as

$$F=\tfrac{1}{2}k_{11}(\nabla\cdot\mathbf{n})^2+\tfrac{1}{2}k_{22}(\mathbf{n}\cdot\nabla\times\mathbf{n})^2+\tfrac{1}{2}k_{33}(\mathbf{n}\times\nabla\times\mathbf{n})^2-\tfrac{1}{2}\varepsilon_0\Delta\varepsilon(\mathbf{n}\cdot\boldsymbol{E})^2, \quad (1)$$

where k_{11}, k_{22}, and k_{33} are elastic constants of LC for splay, twist, and bend deformations, respectively; ε_0 is the vacuum permittivity, $\Delta\varepsilon=\varepsilon_{||}-\varepsilon_\perp$ is the dielectric anisotropy of LC. The most general form for the surface free energy of a nematic is the so-called Rapini-Popoular surface potential

$$f_s=\tfrac{1}{2}W_T\sin^2(\Delta\phi_T)+\tfrac{1}{2}W_B\sin^2(\Delta\phi_B)+\tfrac{1}{2}U_T\sin^2(\Delta\theta_T)+\tfrac{1}{2}U_B\sin^2(\Delta\theta_B). \quad (2)$$

$\Delta\phi$ and $\Delta\theta$ are the azimuthal and polar deviation angles of surface LCs, respectively, from the easy axis at surfaces; T and B represent top and bottom substrates, respectively.

The balance of torques acting on **n** can be expressed by the Ericksen-Leslie equation [1,37,38]:

$$0=\gamma n_i-\frac{\partial F}{\partial n_i}-\gamma_1 N_i-\gamma_2 n_j A_{ij}+\left(\frac{\partial F}{\partial n_{i,j}}\right)_{,j}, \quad (3)$$

where γ_1 and γ_2 are the rotational and shear viscosities, respectively; N_i and A_{ij} are the rotation of **n** relative to the fluid velocity (v_i) and the symmetric parts of v gradient tensor, respectively, which can be written as $\dot{n}_i-1/2(v_{i,j}-v_{j,i})n_j$ and $1/2(v_{i,j}+v_{j,i})$ via the Navier–Stokes equation [1,39]. In

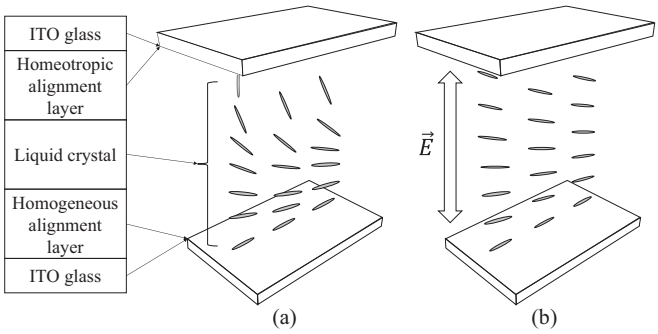

FIG. 1. Schematic illustrations of the LC cell with director profiles (a) before and (b) after the application of vertical electric field ($\boldsymbol{E}$) for determining an unknown azimuthal anchoring energy (W) at homeotropic alignment layer.

Eq. (3), the inertial terms involving the second time-derivative of **n** are neglected. The general flow equation can be written as $\rho\,\dot{v}_i=F_i+\sigma_{ji,j}$, where ρ is the fluid density and the body force $F_i=0$ due to no gravitation. Here, the stress tensor σ_{ji} by LC flow is [1,40]

$$\sigma_{ji}=-P\delta_{ij}-(\partial F/\partial n_{k,j})n_{k,j}+\alpha_1 n_k n_p A_{kp}n_i n_j+\alpha_2 n_j N_i+\alpha_3 n_i N_j+\alpha_4 A_{ij}+\alpha_6 n_i n_k A_{kj}, \quad (4)$$

where P is the hydrostatic pressure (here $P=0$) and α indicates Leslie's coefficients. The second term of Eq. (4) does not apply to the linearized equations because it is a second-order term in the deformation of **n**. By Onsager reciprocity, a relational expression between the coefficients is $\alpha_6-\alpha_5=\alpha_2+\alpha_3$. Therefore, the rotational can be expressed as terms of the shear viscosities, $\gamma_1=\alpha_3-\alpha_2$ and $\gamma_2=\alpha_2+\alpha_3$. Here, the fluid is considered incompressible, so that $\nabla\cdot v=0$. Finally, when the equations are applied to Eq. (3), we can obtain the LC orientation at each position in the LC cell that is dependent on the surface anchoring energies of both substrates. If the surface anchoring energy of one substrate is known, therefore, the corresponding value for the other substrate can be evaluated from Eq. (3) by measuring the orientation of $\mathbf{n}_\mathrm{m}$. We note that all theoretical calculations in this work were performed by LC simulator, TechWiz LCD (SANAYI System Co., LTd.), which can obtain the equilibrium profile of the director minimizing the total free energy after sufficient relaxation of the liquid crystal through the Ericksen-Leslie equation. Here, several calculations should be carried out for many anchoring strengths to find the real anchoring strength that gives the desired midplane orientation (measured midplane orientation). We set the polar anchoring strengths by $5\times10^{-5}\,\mathrm{N/m}$. In fact, the midplane direction remained unchanged at polar anchoring strengths, U_T and U_B above $10^{-5}\,\mathrm{N/m}$ for a fixed azimuthal anchoring strength.

III. EXPERIMENTAL METHOD

The cell was assembled with two indium thin oxide (ITO)-glass substrates that were coated with homeotropic and planar alignment layers. The alignment layers were rubbed perpendicular to each other [red arrows in Fig. 1(a)] to impose a hybrid-twist configuration of LCs as depicted in Fig. 1(a);

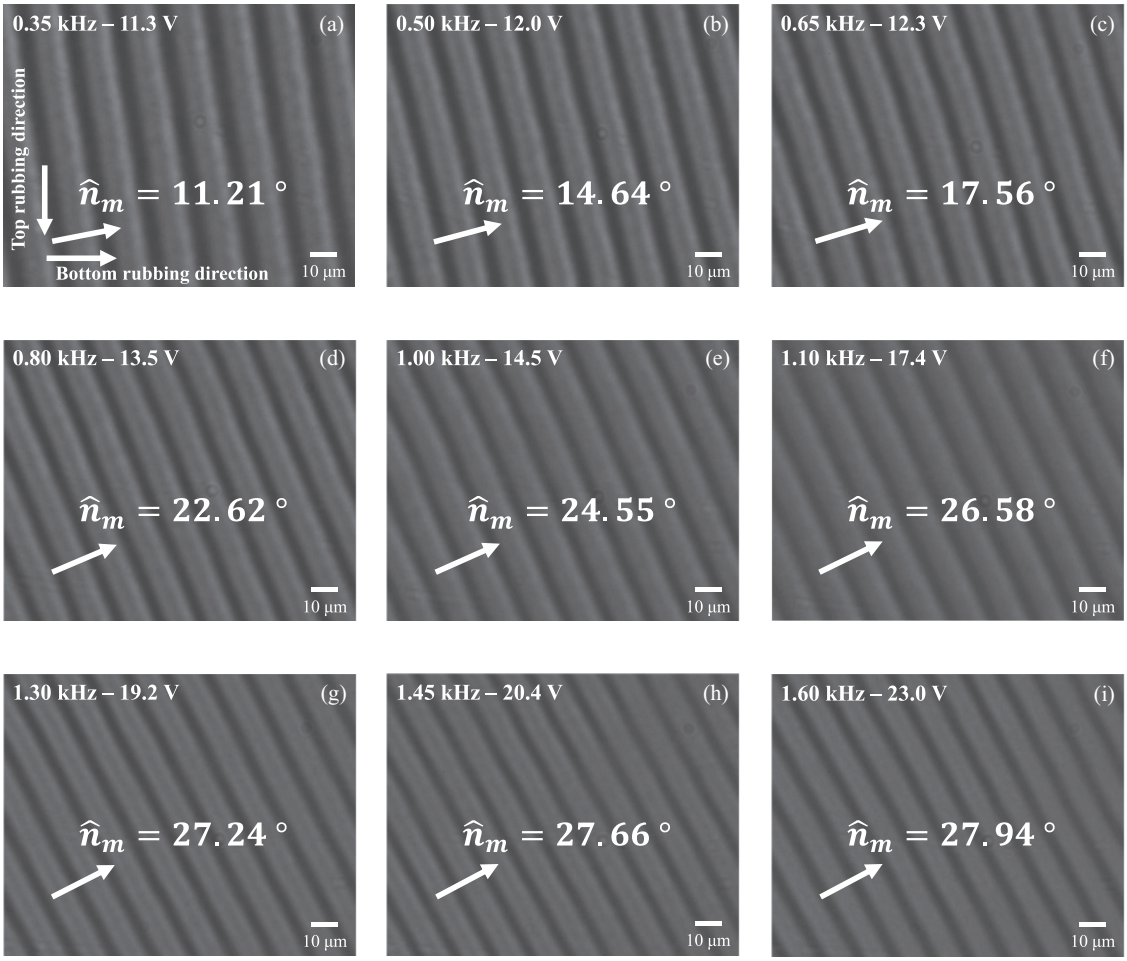

FIG. 2. (a)–(i) Micrographs showing the rotation of roll patterns as a function of frequency and voltage applied to the HTLC-1 cell with the planar alignment layer SE-3140 (bottom substrate) and the vertical alignment layer SE-1211 (top substrate). The substrates were rubbed into the directions denoted in (a). $\mathbf{n}_m$ is director at the midplane of the LC cell.

planar anchoring at one substrate and homeotropic anchoring at the other substrate with 90° twist of **n** across the cell. Under $\boldsymbol{E}$, however, the LC configuration is transformed into a typical twist deformation due to $\Delta\varepsilon < 0$ of the used LC, MBBA is *p*-methoxybenzylidene-*p*-*n*-butylaniline (MBBA).

Figure 1 shows the configuration of LC cells used in this work to determine the unknown W at homeotropic alignment surfaces. The LC cells were comprised of two bounding surfaces imposing a hybrid-twist LC (HTLC) configuration cell as shown in Fig. 1(a); planar anchoring at bottom substrate and homeotropic anchoring at top substrate with 90° twist of **n** across the cell. Specifically, ITO-glass substrates were spin coated with a homeotropic alignment layer SE-1211 (Nissan Chemical) and a planar alignment layer of polyimide SE-3140 for HTLC-1 cells or polyvinyl alcohol (PVA) for HTLC-2 cells. The substrates were rubbed to set a preferred azimuthal orientation of LCs (i.e., easy axis) and assembled in a crossed fashion, Fig. 1(a). The thickness (d) of LC cells was set by glass spacers with a diameter of 8.5 μm. The rubbing conditions were as follows: the rotation speed of rubbing roll was 800 rpm, the rubbing depth was 3 mm, and the speed of rubbing stage was 5 cm/s. Subsequently, the experimental cells were filled with a nematic LC, MBBA which has $\Delta\varepsilon < 0$ ($\varepsilon_\parallel = 4.72$ and $\varepsilon_\perp = 5.25$), $k_{11} = 6.66$ pN, $k_{22} = 4.2$ pN, $k_{33} = 8.61$ pN, $\alpha_1 = -18.1$, $\alpha_2 = -110.4$, $\alpha_3 = -1.1$, $\alpha_4 = 82.6$, $\alpha_5 = 77.9$, $\alpha_6 = -33.6$, and $\sigma_{||}/\sigma_\perp = 1.5$ [36,40]. Following the injection of LCs, the pretilt angles of **n** at both substrates were measured by the crystal rotation method [41] to be $\theta = 88°$ at the homeotropic alignment layer SE-1211, $\theta = 2 \sim 3°$ at SE-3140, and $\theta = 0°$ at PVA. In this work, all experiments for the observation of the roll patterns in the HTLC cells were performed at the temperature $T < 20$ °C.

IV. RESULTS AND DISCUSSION

Figure 2 shows micrographs of the roll patterns induced upon EHC, as a function of the frequency (f) and applied voltage (V) in the HTLC-1 cell with the planar alignment layer SE-3140 and the homeotropic alignment layer SE-1211. Under the conduction region ($V < V_c$ and $f < f_c$), we observed the roll patterns to appear with a spatial periodicity that is dependent on d; V_c and f_c are the critical voltage and frequency, respectively, above which the roll pattern disappear. The critical voltage can be expressed as $V_c = V_0^2(1 + f^2\tau^2)/(\eta^2 - 1 - f^2\tau^2)$, where $V_0 = [-4\pi^3\varepsilon_{ll}/(\varepsilon_{ll} - \varepsilon_\perp)\varepsilon_\perp K_{22}]^{1/2}$, τ is

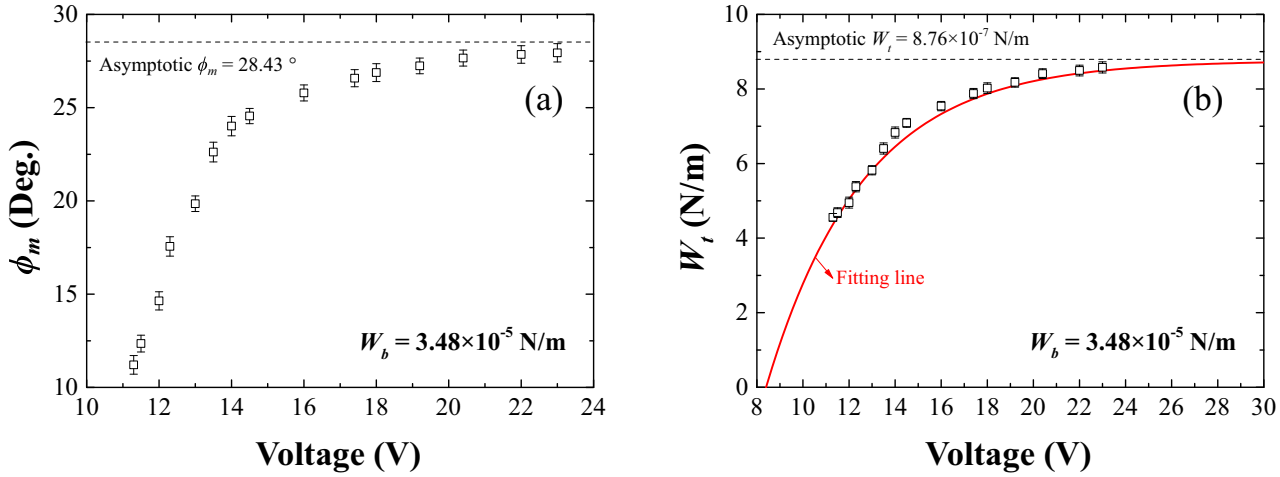

FIG. 3. (a) Measured azimuthal angle ϕ_m of $\mathbf{n}_\mathrm{m}$ and (b) calculated azimuthal anchoring energy W_T of homeotropic alignment layer (SE-1211) with respect to applied voltage in the HTLC-1 cell with the planar alignment layer SE-3140 ($W_B = 3.48 \times 10^{-5}$ N/m). The red fitted line was obtained from Eq. (4).

the dielectric charge relaxation time, and η is a dimensionless coefficient [1]. As shown in Fig. 2(a), at $V = 11.3$ V and $f = 0.35$ kHz, we measured the azimuthal angle (ϕ_m) of mid-plane $\mathbf{n}$ ($\mathbf{n}_\mathrm{m}$) with respect to the rubbing direction of planar alignment layer SE-3140 (bottom substrate) to be 11.21° from the orientation of induced roll pattern (perpendicular to $\mathbf{n}_\mathrm{m}$). By applying the known value of W_B(SE-3140) $= 3.48 \times 10^{-5}$ N/m [18] and measured $\phi_m = 11.2°$ into Eq. (2), we could obtain the unknown W of homeotropic alignment layer to be W_T(SE-1211) $= 4.56 \times 10^{-7}$ N/m. The result is consistent with our observations (Fig. 2) in which $\mathbf{n}_\mathrm{m}$ is inclined towards the easy axis of planar surface, suggesting $W_B \gg W_T$. Additionally, we investigated the dependence of W_T on f and V. Upon increase in f and V from 0.35 kHz, 11.3 V (V_min) to 1.6 kHz, 23 V (V_max), we observed the roll patterns to rotates in anticlockwise direction from $\phi_m = 11.21°$ to 27.94°, Figs. 2(b)–2(i). As plotted in Fig. 3(a), we found ϕ_m to reach the plateau of 28.43° as V increases, and the roll pattern to disappear at 24 V($= V_c$). From the measured values of ϕ_m, therefore, we could evaluate W_T (SE-1211) as a function of V, which shows gradual increase in W_T from 4.56×10^{-7} N/m (at V_min) to 8.58×10^{-7} N/m (at V_max) toward the asymptotic value of $W_T(V = \infty, \theta = 0°) = 8.76 \times 10^{-7}$ N/m, Fig. 3(b). Due to $\Delta\varepsilon < 0$ of the used LC (MBBA), the result indicates that the field-induced transition of surface LCs from the initial homeotropic ($\theta = 90°$) to planar orientation ($\theta = 0°$) causes an increase in W_T (SE-1211).

In Fig. 3(b), the fitting line was obtained from an exponential form:

$$W_T(V) = W_\mathrm{max}(1 - e^{-2(V - V_\mathrm{th})/V_\mathrm{th}}) \quad \text{at} \quad V \geqslant V_\mathrm{th}. \qquad (5)$$

Here, V_th is the threshold voltage above which the polar angle θ of $\mathbf{n}$ changes, and thus be correlated with the polar anchoring energy U of the surface; the stronger U, the higher V_th [1,37]. We note that because V_th can be extrapolated [$V_\mathrm{th} = 8.4$ V in Fig. 3(b)] from the fitting of measured ϕ_m as a function of V using Eq. (4), one can use our approach to measure not only the azimuthal anchoring energy but also the polar anchoring energy in the HTLC cells with negative ($\Delta\varepsilon < 0$) and positive LCs ($\Delta\varepsilon > 0$) for the measurements on U of homeotropic and planar alignment layers, respectively.

To examine the consistency of our measurement on W_T (SE-1211) in the HTLC-1 cell, we reevaluate W_T (SE-1211) in the HTLC-2 cell that has a different planar alignment layer PVA (SE-3140 for HTLC-1 cell). Figure 4 shows micrographs of roll patterns induced in the HTLC-2 cells as a function of f and V. Consistent with the results in Fig. 2, the typical roll patterns were also observed in the HTLC-2 cell under the conduction regime (at $f < f_c$ and $V < V_c$). In HTLC-2 cell, we determined $V_c \sim 19$ V to be lower than that of the HTLC-1 cell ($V_c \sim 24$ V), which results from the weaker surface anchoring of PVA than SE-3140. As shown in Fig. 4(a), at $V = 10.2$ V with $f = 0.65$ kHz, we observed the orientation of roll patterns to be at 115.58° with respect to the rubbing direction on PVA (bottom substrate) and measured $\phi_m = 25.58°$, which suggests W_B(PVA) $> W_T$(SE-1211). W_B(PVA) $= 3.7 \times 10^{-6}$ N/m was reported in previous studies [42,43]. By applying $\phi_m = 25.58°$ into Eq. (2), therefore, we obtain W_T(SE-1211) $= 2.64 \times 10^{-7}$ N/m.

We also investigated the rotation of roll patterns in the HTLC-2 cell upon increase of V from 10.2 V ($f = 0.65$ kHz) to 19.0 V ($f = 1.55$ kHz) within the conduction regime, and measured corresponding ϕ_m to change from 25.58° [Fig. 4(a)] to 31.55° [Fig. 4(i)], respectively, toward the asymptotic $\phi_m(V = \infty, \theta = 0°) = 32.41°$ as plotted in Fig. 5(a). We subsequently evaluated W_T (SE-1211) from the measured values of ϕ_m in the HTLC-2 cell and confirmed a similar trend [Fig. 5(b)] to the previously results obtained from the HTLC-1 cells [Fig. 3(b)]; as V increases, W_T (SE-1211) is gradually enhanced and eventually reaches the plateau. When fitted using Eq. (4), W_T (SE-1211) was shown to be saturated at $W_T(V = \infty, \theta = 0°) = 8.75 \times 10^{-7}$ N/m in the HTLC-2 cell [(Fig. 5(b)], which is in excellent agreement with the asymptotic value of $W_T(V = \infty, \theta = 0°) = 8.76 \times 10^{-7}$ N/m obtained from the HTLC-1 cell [Fig. 3(b)]. In addition, we

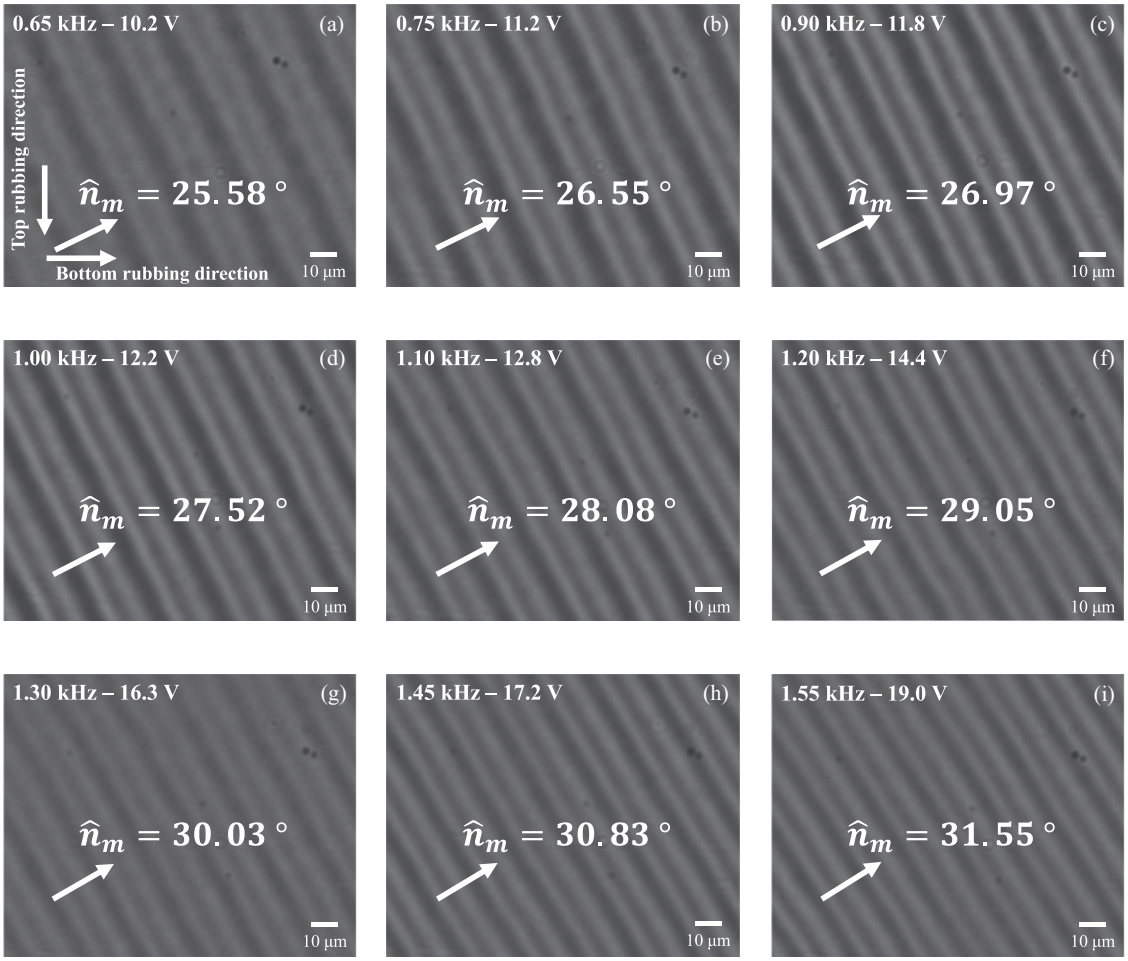

FIG. 4. (a)–(i) Micrographs showing the rotation of roll patterns as a function of frequency and voltage applied to the HTLC-2 cell with the planar alignment layer PVA (bottom substrate) and the vertical alignment layer SE-1211 (top substrate). The substrates were rubbed into the directions denoted in (a).

found the extrapolated $V_{\text{th}} = 8.5\,\text{V}$ from the HTLC-2 cell [Fig. 5(b)] to be also consistent with $V_{\text{th}} = 8.4\,\text{V}$ obtained from the HTLC-1 cell [Fig. 3(b))]. These results demonstrate excellence in our methodology that is significantly accurate, yet simple and easy to measure the azimuthal anchoring energy between LCs and surfaces.

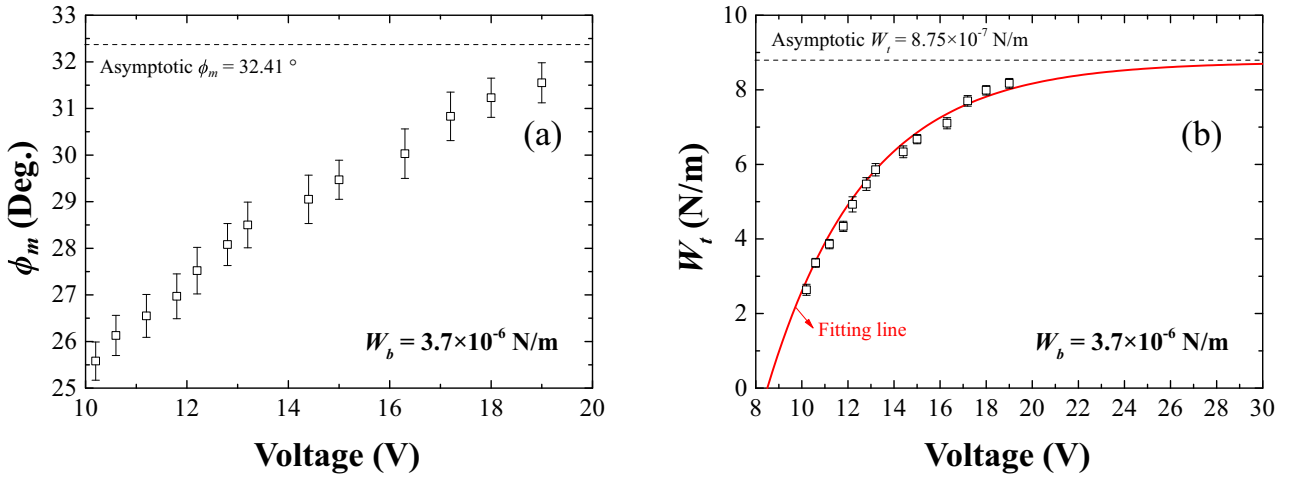

FIG. 5. (a) Measured azimuthal angle ϕ_m of midplane **n** and (b) calculated azimuthal anchoring energy W_T of homeotropic alignment layer (SE-1211) with respect to applied voltage in the HTLC-2 cell with the planar alignment layer PVA ($W_B = 3.7 \times 10^{-6}\,\text{N/m}$). The red fitted line was obtained from Eq. (4).

V. CONCLUSIONS

We presented a technique to determine the azimuthal anchoring energy, with respect to the polar angle, of the surface LCs of initially homeotropic LC alignment, using the Williams convection roll pattern of the conduction regime of the electrohydrodynamic convection patterns of LCs. The midplane LC directions, obtained from the direction of the roll patterns, provide approximate information about surface anchoring strengths. The application of those values to the Ericksen-Leslie equation provides the precise values of the anchoring strength. The hybrid type 90° twisted nematic (HTN) LC cell, composed of homeotropic and homogeneous LC alignment films on the top and bottom substrates, respectively, was used to find the azimuthal anchoring energy of the surface LCs, with respect to the voltages at initially homeotropic LC alignment. It was observed that the surface azimuthal anchoring energy on the homeotropic layer increased with an increase in voltage, however, the amount by which the values increased gradually decreased. The threshold voltage V_{th}, that causes LCs fixed on T to start moving, is determined from the fitted results of the surface azimuthal anchoring energies, dependent on voltage. It may determine the polar anchoring energy of vertically aligned liquid crystal (VALC), by relation to this threshold voltage in the HTN cell with negative dielectric anisotropic LCs, satisfying the conditions for EHC. We expect that the proposed technique may be excellent in terms of ease, simplicity, and accuracy because the azimuthal anchoring energy can be visually evaluated.

ACKNOWLEDGMENTS

This work was supported through the Basic Science Research Program through the National Research Foundation of Korea (NRF) funded by the Ministry of Science, ICT, and Future Planning (Grant No. 2019R1D1A3A03103662).

[1] P. G. de Gennes and J. Prost, *The Physics of Liquid Crystals* (Clarendon Press, Oxford, 1993).
[2] M. Kleman and O. D. Lavrentovich, *Soft Matter Physics: An Introduction* (Springer, New York, 2003).
[3] Y.-K. Kim, J. Noh, K. Nayani, and N. L. Abbott, Soft Matter **15**, 6913 (2019).
[4] E. Bukusoglu, M. B. Pantoja, P. C. Mushenheim, X. Wang, and N. L. Abbott, Annu. Rev. Chem. Biomol. Eng. **7**, 163 (2016).
[5] P. Popov, E. K. Mann, and A. Jakli, J. Mater. Chem. B **5**, 5061 (2017).
[6] Y.-K. Kim, X. Wang, P. Mondkar, E. Bukusoglu, and N. L. Abbott, Nature (London) **557**, 539 (2018).
[7] D.-K. Yang and S.-T. Wu, *Fundamentals of Liquid Crystal Devices* (Wiley, Chichester, 2006).
[8] X. W. Shield IV, Y.-K. Kim, K. Han, A. C. Murphy, A. J. Scott, N. L. Abbott, and O. D. Velev, Adv. Intell. Syst. **2**, 1900114 (2020).
[9] H. K. Bisoyi, T. J. Bunning, and Q. Li, Adv. Mater. **30**, 1706512 (2018).
[10] A. H. Gelebart, D. J. Mulder, M. Varga, A. Konya, G. Vantomme, E. W. Meijer, R. L. B. Selinger, and D. J. Broer, Nature (London) **546**, 632 (2017).
[11] H. K. Bisoyi and Q. Li, Chem. Rev. **116**, 15089 (2016).
[12] G. J. Choi, Q. V. Le, K. S. Choi, K. C. Kwon, H. W. Jang, J. S. Gwag, and S. Y. Kim, Adv. Mater. **29**, 1702598 (2017).
[13] K. Nayani, P. Rai, N. Bao, H. Yu, M. Mavrikakis, R. J. Twieg, and N. L. Abbott, Adv. Mater. **30**, 1706707 (2018).
[14] J. S. Gwag, J. Yi, and J. H. Kwon, Opt. Lett. **35**, 456 (2010).
[15] T. Govindaraju, P. J. Bertics, R. T. Raines, and N. L. Abbott, J. Am. Chem. Soc. **129**, 11223 (2007).
[16] B. H. Clare, O. Guzman, J. de Pablo, and N. L. Abbott, Langmuir **22**, 7776 (2006).
[17] B. H. Clare, O. Guzman, J. J. de Pablo, and N. L. Abbott, Langmuir **22**, 4654 (2006).
[18] J. S. Gwag, S. J. Kim, J. G. You, J. Y. Lee, J. C. Kim, and T. H. Yoon, Opt. Lett. **30**, 1387 (2005).
[19] Y. Saitoh and A. Lien, Jpn. J. Appl. Phys. **39**, 1743 (2000).
[20] F. Z. Yang, L. Z. Ruan, and J. R. Sambles, J. Appl. Phys. **88**, 6175 (2000).
[21] Y. Ohno, T. Ishinabe, T. Miyashita, and T. Uchida, Jpn. J. Appl. Phys. **47**, 969 (2008).
[22] Y. A. Nastishin, R. D. Polak, S. V. Shiyanovskii, V. H. Bodnar, and O. D. Lavrentovich, J. Appl. Phys. **86**, 4199 (1999).
[23] Y. A. Nastishin, R. D. Polak, S. V. Shiyanovskii, and O. D. Lavrentovich, Appl. Phys. Lett. **75**, 202 (1999).
[24] D. Subacius, V. M. Pergamenshchik, and O. D. Lavrentovich, Appl. Phys. Lett. **67**, 214 (1995).
[25] D. F. Gu, S. Uran, and C. Rosenblatt, Liq. Cryst. **19**, 427 (1995).
[26] J. H. Huh, Phys. Rev. E **92**, 062504 (2015).
[27] T. Toth-Katona, N. Eber, and A. Buka, Phys. Rev. E **83**, 061704 (2011).
[28] T. Toth-Katona and J. T. Gleeson, Phys. Rev. E **69**, 016302 (2004).
[29] J. H. Huh, Y. Yusuf, Y. Hidaka, and S. Kai, Phys. Rev. E **66**, 031705 (2002).
[30] J. H. Huh, Y. Hidaka, A. G. Rossberg, and S. Kai, Phys. Rev. E **61**, 2769 (2000).
[31] L. Kramer and W. Pesch, Annu. Rev. Fluid Mech. **27**, 515 (1995).
[32] W. Helfrich, J. Chem. Phys. **51**, 4092 (1969).
[33] C. G. Jhun, G. J. Choi, D. G. Ryu, J. H. Huh, and J. S. Gwag, Phys. Rev. E **98**, 052704 (2018).
[34] G. J. Choi, J. M. Song, C. G. Jhun, J.-H. Huh, and J. S. Gwag, Phys. Rev. E **96**, 040701(R) (2017).
[35] V. A. Delev, P. Toth, and A. P. Krekhov, Mol. Cryst. Liq. Cryst. **351**, 179 (2000).
[36] A. Hertrich, A. P. Krekhov, and O. A. Scaldin, J. Phys. II France **4**, 239 (1994).
[37] D. Demus, J. Goodby, G. W. Gray, H.-W. Spiess, and V. Vill, *Handbook of Liquid Crystals* (Wiley-VCH Verlag GmbH, New York, 1998).
[38] F. M. Leslie, Adv. Liq. Cryst. **4**, 1 (1979).
[39] D. J. Tritton, *Physical Fluid Dynamics* (Clarendon Press, Oxford, 1988).

[40] E. Bodenschatz, W. Zimmermann, and L. Kramer, J. Phys.-Paris **49**, 1875 (1988).

[41] J. S. Gwag, S. H. Lee, K. H. Park, W. S. Park, K. Y. Han, C. G. Jhun, T. H. Yoon, J. C. Kim, D. M. Song, and D. M. Shin, J. Appl. Phys. **93**, 4936 (2003).

[42] G. J. Choi, D. G. Ryu, J. S. Gwag, Y. Choi, T. H. Kim, M. S. Park, I. Park, J. W. Lee, and J. G. Park, J. Appl. Phys. **125**, 064501 (2019).

[43] Y. Zhou, Z. He, and S. Sato, Jpn. J. Appl. Phys. **38**, 4857 (1999).